



Alligat0R: Pre-Training through Co-Visibility Segmentation for Relative Camera Pose Regression

Thibaut Loiseau¹ Guillaume Bourmaud² Vincent Lepetit¹

¹ LIGM, Ecole des Ponts, Univ Gustave Eiffel, CNRS, France

² Laboratoire IMS, Université de Bordeaux, France

{thibaut.loiseau, vincent.lepetit}@enpc.fr guillaume.bourmaud@u-bordeaux.fr

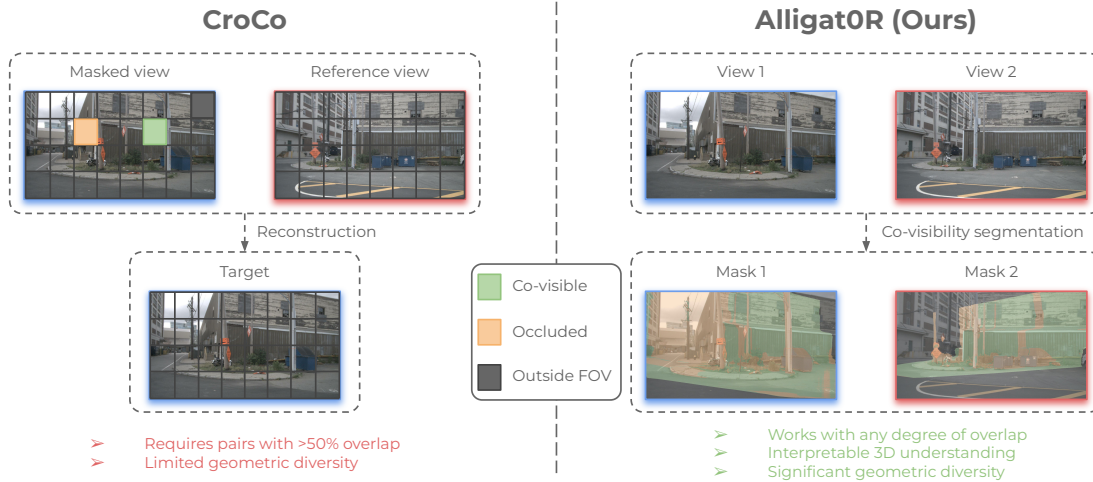


Figure 1. **We introduce Alligat0R, a pretraining method for binocular vision robust to wide baselines.** Alligat0R explicitly segments pixels as **co-visible**, **occluded**, or outside field-of-view, overcoming the fundamental limitation of CroCo [45, 46] which attempts to reconstruct potentially unobservable regions. We demonstrate Alligat0R on relative pose regression and show that it allows us to significantly outperform the state-of-the-art, especially on pairs with very low overlap.

Abstract

Pre-training techniques have greatly advanced computer vision, with CroCo’s cross-view completion approach yielding impressive results in tasks like 3D reconstruction and pose regression. However, this method requires substantial overlap between training pairs, limiting its effectiveness. We introduce Alligat0R, a novel pre-training approach that reformulates cross-view learning as a co-visibility segmentation task. Our method predicts whether each pixel in one image is co-visible in the second image, occluded, or outside the field of view (FOV), enabling the use of image pairs with any degree of overlap and providing interpretable predictions. To support this, we present Cub3, a large-scale dataset with 2.5 million image pairs and dense co-visibility annotations derived from the nuScenes dataset. This dataset includes diverse scenarios with varying degrees of overlap. The experiments show that Alligat0R significantly outperforms CroCo in relative pose regression, especially in scenarios with limited overlap. Alligat0R and Cub3 will be made publicly available.

1. Introduction

Pre-training techniques have revolutionized computer vision by enabling large models to learn rich representations [1, 3, 5, 16, 17, 28, 53]. In 3D computer vision, CroCo [45, 46] pioneered cross-view completion as a pretext task, where one view is partially masked and reconstructed using visible portions along with a second reference view of the same scene (see Fig. 1 left). This approach allows to learn powerful 3D features and has made possible impressive results on downstream tasks such as 3D reconstruction [12, 40, 43, 47], 3D pose regression [7], camera calibration [24], 4D reconstruction [21, 42, 50] and Gaussian splatting [33, 49].

Despite its success, the cross-view completion pretext task has a fundamental limitation: pretraining is only effective when training pairs have substantial overlap. For instance, CroCo [45, 46] relies on pairs with at least 50% overlap. We are particularly interested in relative pose regression between two images, and using this pretext task impairs the performance of pose regression on pairs with limited overlap, as our results show.

In this paper, we present Alligat0R (see Fig. 1 right), a novel pre-training approach that reformulates the cross-view learning objective as a co-visibility segmentation task. Instead of reconstructing masked regions, our method explicitly predicts whether each pixel in one image is: (1) co-visible in the second image, (2) occluded, or (3) outside the field of view (FOV). This formulation offers several advantages: it can use image pairs with any degree of overlap, it provides interpretable predictions that reveal the model’s geometric understanding, and it aligns more directly with the correspondence reasoning required in downstream binocular vision tasks.

To enable our approach, we introduce Cub3, a large-scale dataset comprising 2.5 million image pairs with dense co-visibility annotations derived from the nuScenes dataset. This dataset includes challenging scenarios with varying degrees of overlap between views, providing a more diverse training signal than previous approaches.

One might notice that Alligat0R is not strictly self-supervised, unlike some earlier pre-training methods, as it relies on co-visibility annotations. However, the same can be said for CroCo, which requires filtering image pairs to retain only those with at least 50% overlap. The creation of our co-visibility annotations is more complex than for CroCo’s, however the process is fully automated. This process is very similar to the one used in RUBIK [26] and relies on registered video sequences and depth predictions.

Our contributions can be summarized as follows:

1. We introduce co-visibility segmentation as a novel pre-training objective for binocular vision tasks, replacing the cross-completion-based approach of prior work while maintaining the same architecture.
2. We demonstrate that co-visibility segmentation-based pretraining significantly benefits from its ability to learn from challenging image pairs, *i.e.* from any overlap.
3. We create and release Cub3, a large-scale dataset with dense co-visibility annotations derived from the nuScenes dataset.
4. We show that Alligat0R significantly outperforms CroCo pre-training when fine-tuned on the relative pose regression task, particularly for challenging scenarios with limited overlap between views.
5. We demonstrate the effectiveness of our learning based on geometric difficulty and provide insights into the model’s cross-view reasoning capabilities through interpretable segmentation outputs.

Our experiments demonstrate that explicitly learning to understand co-visibility relationships between image pairs leads to more robust and transferable features for relative pose regression compared to reconstruction-based approaches.

2. Related Work

Pretraining on Image Pairs. To the best of our knowledge, CroCo [45] pioneered the extension of masked image modeling [18] to image pairs, introducing cross-view completion. CroCo v2 [46] applied this cross-view completion framework to large amounts of data. P-Match [54] introduced a variation where both images are partially masked to pre-train an image matching model. Another variant, masked appearance transfer, was proposed in [51] for object tracking, with a similar approach in [34]. Let us highlight that the foundational models DUST3R [43] and MAST3R [24] are built on CroCo. While all these works rely on cross-view completion, we depart from this framework and propose a novel pretraining objective based on co-visibility segmentation.

Considering co-visibility across image pairs. Ground-truth co-visibility masks are widely used in image matching methods [4, 9–11, 13–15, 20, 23, 25, 30, 31, 35–37, 41, 44, 52] to compute overlaps and select training pairs. Several approaches [9, 11, 14, 31, 38] also leverage these masks to learn *matchability* scores, which are used at test time to select correspondences. Additionally, [19] jointly learns co-visibility and relative planar pose between 360° panoramas. To the best of our knowledge, our work is the first to learn visual representations from co-visibility segmentation.

Fine-tuning for Relative Pose Regression. Reloc3R [7] recently fine-tuned the foundational model DUST3R [43], which is based on CroCo, on large-scale data for relative pose regression. In our experiments, we adopt a similar strategy to evaluate our novel pretraining method against CroCo. However, we focus on the autonomous driving scenario with metric relative translation, whereas Reloc3R predicts only the direction of the relative translation.

3. Method

In this section, we describe our novel pre-training approach, Alligat0R, which replaces the cross-view completion objective used in CroCo [45, 46] by a segmentation task. We first outline the overall architecture, which remains largely similar to CroCo, and then detail our co-visibility segmentation pre-training objective. Finally, we explain how our model can be fine-tuned for downstream tasks such as relative pose regression.

3.1. Architecture Overview

Our architecture closely follows the design of CroCo, which consists of an encoder and a decoder. The encoder is a ViT [8] that processes the input images by dividing them into non-overlapping patches and encoding them into feature representations. The decoder is another transformer

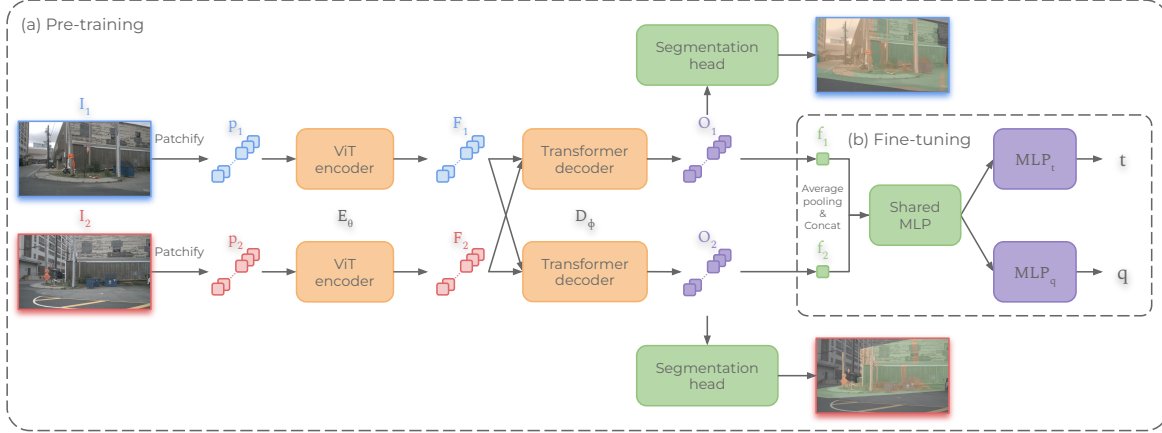


Figure 2. **Overview of Alligat0R.** (a) During pre-training, we use the same architecture as CroCo but replace the reconstruction objective with a co-visibility segmentation task, without masking, where each pixel in one view is classified as **co-visible**, **occluded**, or **outside FOV** with respect to the other view. (b) For fine-tuning on the relative pose regression task, we pool features from both views, process them through a shared MLP, and use separate heads for predicting translation and rotation.

that combines information from both views, using cross-attention layers, to make predictions.

We adopt a symmetric architecture for our forward pass, where both images are processed in the same way without any masking. This differs from CroCo, which uses an asymmetric approach that heavily masks one image while leaving the other unmasked. Our symmetric design is not only more efficient but also better aligned with downstream binocular vision tasks, which typically process unmasked images.

As shown in Fig. 2 (a), given two images I_1 and I_2 of the same scene taken from different viewpoints, we first divide both into non-overlapping patches, denoted as tokens $p_1 = \{p_1^1, \dots, p_1^{N_1}\}$ and $p_2 = \{p_2^1, \dots, p_2^{N_2}\}$.

The encoder E_θ processes the tokens from both images independently:

$$F_1 = E_\theta(p_1), \quad F_2 = E_\theta(p_2), \quad (1)$$

and the decoder D_ϕ then takes these features and processes them to enable cross-view reasoning:

$$O_1 = D_\phi(F_1, F_2), \quad O_2 = D_\phi(F_2, F_1), \quad (2)$$

where O_1 and O_2 represent the output features from the decoder. The decoder contains cross-attention mechanisms that allow information exchange between features from both views.

3.2. Co-Visibility Segmentation Pre-Training

A key difference between our approach and CroCo lies in the pre-training objective. Instead of reconstructing masked pixels, we formulate the pre-training task as a co-visibility segmentation problem. Our goal is to predict for each pixel in each image whether it is:

1. **Co-visible:** the pixel corresponds to a 3D point that is also visible in the other image.
2. **Occluded:** the pixel corresponds to a 3D point that is occluded in the other image.
3. **Outside FOV:** the pixel corresponds to a 3D point that is outside the field of view in the other image.

Formally, for each patch token, the decoder produces a feature vector that is processed by a fully-connected layer to output probabilities for each of the three classes, for each pixel:

$$\hat{y}_{ikj} = \text{softmax}(W \cdot O_{ik} + b)_j, \quad (3)$$

where $\hat{y}_{ikj} \in \mathbb{R}^3$ represents the predicted probabilities for the three co-visibility classes for pixel j in patch k of image i , and W and b are learnable parameters.

During pre-training, we optimize the network using a cross-entropy loss in each image:

$$\mathcal{L}_{ce_i} = -\frac{1}{N_i} \sum_{j=1}^{N_i} \log(\hat{y}_{ij, c_{ij}}), \quad (4)$$

where c_{ij} is the ground-truth class in pixel j of image i , and N_i is the number of pixels in each image.

This formulation offers several advantages over the cross-view-completion-based approach. First, it allows us to use image pairs with any degree of overlap, as we explicitly model cases where pixels have no co-visible region in the other view. Second, it provides interpretable outputs that directly reveal the model’s understanding of scene geometry. Third, it better aligns with downstream tasks such as pose regression, where both images are fully visible.

3.3. Fine-Tuning for Relative Pose Regression

After pre-training, we fine-tune our model for the task of relative pose regression. We add a pose regression head on top of the pre-trained encoder-decoder architecture, while keeping the original co-visibility segmentation head. This design allows the model to leverage the geometric understanding acquired during pre-training.

The pose regression head consists of several components as shown in Fig. 2 (b). First, we apply global average pooling to the decoder outputs for both images:

$$f_1 = \text{GlobalAvgPool}(O_1), \quad f_2 = \text{GlobalAvgPool}(O_2). \quad (5)$$

The pooled features are concatenated and processed through a shared MLP:

$$f_{\text{shared}} = \text{MLP}([f_1, f_2]). \quad (6)$$

We then use separate heads for predicting the metric relative translation vector $t \in \mathbb{R}^3$ and the relative rotation represented as a quaternion $q \in \mathbb{R}^4$:

$$t = \text{MLP}_t(f_{\text{shared}}), \quad q = \text{MLP}_q(f_{\text{shared}}). \quad (7)$$

Our fine-tuning stage consists of two phases:

1. First, we freeze the pre-trained encoder, decoder and co-visibility segmentation head, and only train the pose regression head. During this phase, we use a homoscedastic loss [22] combining MSE losses for translation and quaternion predictions:

$$\mathcal{L}_{\text{pose}} = \frac{1}{2\sigma_t^2} \|t - \hat{t}\|^2 + \frac{1}{2\sigma_q^2} \|q - \hat{q}\|^2 + \log \sigma_t + \log \sigma_q, \quad (8)$$

where t and q are the ground-truth metric translation and quaternion respectively, and σ_t and σ_q are learnable parameters that automatically balance the two loss terms.

2. In the second phase, we unfreeze the backbone and the co-visibility segmentation head, and train the full network with a joint loss that combines the pose regression loss and the co-visibility segmentation loss:

$$\mathcal{L}_{\text{joint}} = \frac{1}{2\sigma_{\text{pose}}^2} \mathcal{L}_{\text{pose}} + \frac{1}{2\sigma_{\text{seg}}^2} \mathcal{L}_{\text{ce}} + \log \sigma_{\text{pose}} + \log \sigma_{\text{seg}}, \quad (9)$$

where σ_{pose} and σ_{seg} are learnable parameters that balance the two loss components.

This training strategy ensures that the model maintains its interpretable co-visibility segmentation capabilities while being optimized for the pose regression task.

4. Cub3: A Large-Scale Co-Visibility Dataset

To enable our co-visibility segmentation approach, we introduce Cub3, a large-scale dataset comprising 2.5 million image pairs with dense co-visibility annotations derived from the autonomous driving nuScenes dataset [2]. Cub3 will be made publicly available.

4.1. Dataset Construction

We leverage the co-visibility estimation pipeline introduced in RUBIK [26] to generate pixel-level co-visibility annotations for image pairs. In brief, this pipeline uses monocular metric depth predictions from UniDepth [29] and surface normals from Depth Anything V2 [48], combined with camera poses from COLMAP [32] reconstructions, to automatically classify each pixel as either co-visible, occluded, or outside FOV with respect to another image.

Starting from the nuScenes training set, we apply this pipeline to all possible image pairs within each scene, resulting in approximately 34 million annotated pairs. For our experiments, we created two dataset variants, each containing 2.5 million image pairs:

- **Cub3-50:** Image pairs with at least 50% overlap, similar to the criterion used in CroCo [46]. This dataset provides a direct comparison point with existing cross-view completion approaches.
- **Cub3-all:** Image pairs with at least 5% overlap. This dataset, contains challenging image pairs to test the robustness of methods to handle low-overlap scenarios that are common in real-world applications.

Fig. 3 shows examples of our co-visibility annotations on image pairs from Cub3, illustrating how our process classifies pixels into the three categories across varying levels of difficulty.

It is also worth noting that our annotation process inherits some limitations from the underlying monocular depth estimation models. The depth predictions may occasionally struggle with challenging scenarios such as reflective surfaces, transparent objects, or regions with complex geometry or far-away objects. Consequently, some annotations in our dataset, particularly the distinction between co-visible and occluded pixels, may contain noise. Despite these imperfections, our experiments show that the scale and diversity of Cub3 enable effective training of robust co-visibility segmentation models.

4.2. Dataset Statistics

Fig. 4 illustrates the distribution of our datasets across three geometric criteria introduced in RUBIK: overlap percentage, scale ratio, and viewpoint angle. The Cub3-all dataset’s distribution is heavily skewed towards very challenging pairs, which are particularly difficult for cross-completion methods like CroCo. In contrast, our co-visibility segmentation approach is designed to benefit from such challenging cases effectively.

Given our computational resources, Cub3 is currently limited to autonomous driving scenarios from nuScenes. But such scenarios have very important applications, and given its size, variety, and challenges, Cub3 is already sufficient to validate Alligat0R—very much like the initial



Figure 3. Co-visibility annotation examples from Cub3. For each image pair, we show the corresponding co-visibility maps with color-coding for **co-visible**, **occluded**, and **outside FOV** regions. Note how our annotation process handles varying degrees of overlap and challenging viewpoint changes. Let us highlight that some annotations, particularly the distinction between co-visible and occluded pixels, may contain noise, see text for details.

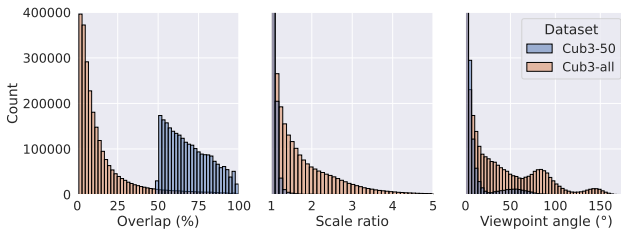


Figure 4. Distributions of overlap, scale ratio, and viewpoint angle in Cub3-all and Cub3-50.

version of CroCo [45] was demonstrated as a “proof-of-concept”:

- **Scale:** With 2.5 million annotated pairs, Cub3 provides sufficient data to train and validate our approach.
- **Geometric variety:** It covers a wide range of overlaps, scales and viewpoint angles within the driving context.
- **Challenging scenarios:** It includes pairs with minimal overlap that test the limits of CroCo, as was done in the original paper.
- **Application relevance:** Autonomous driving represents an important application domain with significant research interest.

Our experiments on the RUBIK benchmark, which was specifically designed to evaluate challenging autonomous driving scenarios, demonstrate the effectiveness of our approach. The promising results we obtain motivate future work to extend Cub3 to more diverse environments beyond urban driving scenes. However, even within this specific domain, our method shows significant improvements over CroCo, particularly in geometrically challenging configurations.

5. Experiments

5.1. Implementation Details

We implement Alligat0R using PyTorch and conduct all experiments on NVIDIA A100 GPUs. The model architecture follows the design described in Sec. 3.1, utilizing a ViT-based encoder and transformer decoder backbone similar to CroCo, with 24 layers for the encoder and 12 for the decoder. The input images are resized to have a maximum dimension of 512 pixels while maintaining their aspect ratio, resulting in an input resolution suitable for capturing sufficient detail while remaining computationally efficient. For pre-training, we use the AdamW optimizer with a learning rate of $1.5e-4$, weight decay of 0.05, and a batch size of 32 per GPU. We employ a cosine learning rate schedule with 2 epochs of warmup and train for 25 epochs on our Cub3 datasets.

For fine-tuning on relative pose regression, we follow the two-phase approach described in Sec. 3.3. In the first phase, we freeze the backbone and train only the pose regression head for 5 epochs with a learning rate of $1e-4$. In the second phase, we unfreeze the entire network and jointly train with both the pose regression loss and co-visibility segmentation loss for an additional 10 epochs with a learning rate of $5e-5$.

The comprehensive architecture of Alligat0R is illustrated in Fig. 2, showing both the pre-training and fine-tuning phases. During pre-training, the model learns to segment pixels in each view as co-visible, occluded, or outside the field of view with respect to the other view. During fine-tuning, we introduce a pose regression head while maintaining the segmentation capability to leverage the geometric understanding acquired during pre-training.

Table 1. Results on RUBIK [26] Benchmark for Relative Pose Regression. See text for details.

Pre-training	Training set	Backbone	Finetune set	5° / 2m	10° / 5m	AUC @ 5/10/20
CroCo	Cub3-50	❄️	Cub3-50	19.10	28.80	15.6 / 24.7 / 33.9
CroCo	Cub3-all	❄️	Cub3-all	8.90	25.20	8.5 / 22.0 / 40.8
Alligat0R	Cub3-50	❄️	Cub3-50	24.40	32.10	14.8 / 23.1 / 31.2
Alligat0R	Cub3-all	❄️	Cub3-all	<u>55.30</u>	<u>82.30</u>	<u>31.1 / 54.0 / 71.8</u>
Alligat0R	Cub3-all	🔥	Cub3-all	60.30	81.90	41.6 / 61.2 / 75.5
From scratch	-	🔥	Cub3-all	29.10	52.30	27.1 / 43.7 / 58.7

5.2. Main Results

Relative Pose Regression Performance. We evaluate our proposed Alligat0R pre-training approach on the relative pose regression task and compare it with CroCo pre-training using the same architecture and fine-tuning protocol. Tab. 1 presents the results on the RUBIK [26] benchmark, which is specifically designed to evaluate performance across different geometric challenges in autonomous driving scenarios.

As shown in Tab. 1, Alligat0R consistently outperforms CroCo across different training and evaluation configurations. Notably, when pre-trained on Cub3-all and fine-tuned with the backbone frozen, Alligat0R achieves significantly higher performance and reaches state-of-the-art on the RUBIK benchmark (55.30% success rate at 5°/2m and 82.30% at 10°/5m) compared to the CroCo model pre-trained on the same dataset (which only achieves 8.90% and 25.20% respectively in the frozen backbone configuration), confirming the results in the original CroCo paper. This substantial improvement demonstrates the effectiveness of our co-visibility segmentation pre-training approach, especially for challenging scenarios with varying degrees of overlap.

Impact of Training Data Distribution. Our results reveal an interesting pattern regarding the impact of training data distribution. When trained on pairs with at least 50% overlap, CroCo achieves modest performance (19.10% accuracy at 5°/2m and 28.80% at 10°/5m). However, when training on the full distribution, Alligat0R shows remarkable improvement (from 24.40% to 55.30% at 5°/2m and from 32.10% to 82.30% at 10°/5m). This confirms our hypothesis that explicitly modeling co-visibility through segmentation enables more effective learning from challenging image pairs with limited overlap.

Fig. 5 further illustrates this advantage by breaking down performance across different overlap percentages, scale ratios and viewpoint angles. While both methods perform well on high-overlap pairs (80-100%), Alligat0R trained on Cub3-all maintains strong performance even as overlap decreases, whereas CroCo’s accuracy drops dramatically for pairs with less than 40% overlap. This demonstrates Alligat0R’s ability to generalize across a wide range of geometric configurations, which is crucial for real-world applications where overlap cannot be guaranteed.

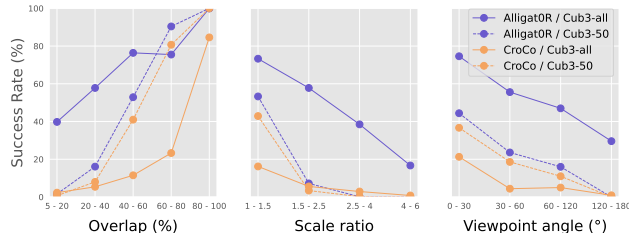


Figure 5. Performance of CroCo and Alligat0R across different geometric challenges. Results show accuracy at the 5°/2m threshold for models trained on different datasets (Cub3-50 or Cub3-all) and for frozen backbones. Alligat0R trained on Cub3-all consistently outperforms other configurations, particularly for challenging cases with low overlap, large scale differences, and extreme viewpoint changes.

Fine-tuning Strategy Comparison. We also compare different fine-tuning strategies, specifically the impact of freezing versus unfreezing the backbone during fine-tuning. For Alligat0R, unfreezing the backbone during fine-tuning leads to even better performance and yielding the best results (60.30% at 5°/2m and 81.90% at 10°/5m compared to 55.30% and 82.30% with the frozen backbone), suggesting that our pre-training approach learns transferable features that can be effectively adapted to the pose regression task.

Comparison with Training from Scratch. To isolate the impact of our pre-training approach, we compare the performance of a model trained from scratch for relative pose regression versus those initialized with Alligat0R or CroCo pre-training. The final row in Tab. 1 shows that training from scratch achieves notably lower performance (29.10% at 5°/2m and 52.30% at 10°/5m) compared to our pre-trained models trained on the same dataset (Cub3-all), highlighting the value of the representations learned during pre-training.

5.3. Qualitative Analysis

Co-visibility and Reconstruction Visualization. Fig. 6 shows qualitative examples of the co-visibility segmentation and CroCo reconstructions produced by our models on pairs from RUBIK. Alligat0R successfully identifies co-visible regions, occluded areas, and regions outside FOV

Table 2. **RUBIK Benchmark.** The results are reported from [26]. Success rate (in %) for each method across individual geometric criterion bins. Best and second-best values for each column are shown in **bold** and underlined respectively.

	Overlap (%)					Scale Ratio				Viewpoint Angle (°)				Whole Dataset	Time (ms)
	80–100	60–80	40–60	20–40	5–20	1.0–1.5	1.5–2.5	2.5–4.0	4.0–6.0	0–30	30–60	60–120	120–180		
<i>Detector-based methods</i>															
ALIKED+LightGlue [52]	53.4	95.8	68.2	38.0	12.7	62.0	31.0	13.1	1.6	50.6	46.0	28.3	2.0	36.8	<u>45</u>
DISK+LightGlue [39]	54.2	91.4	65.9	38.7	11.8	60.4	30.8	11.6	2.4	50.3	43.8	27.4	2.7	35.9	69
SP+LightGlue [6]	64.8	93.3	68.0	36.4	10.9	61.2	28.4	12.5	1.4	49.9	43.0	28.2	0.9	35.7	43
SIFT+LightGlue [27]	68.2	92.1	61.4	32.3	9.9	57.3	26.9	9.6	1.7	49.8	39.7	23.7	0.5	33.1	194
DeDoDe v2 [10]	89.8	93.3	54.8	26.7	7.9	60.4	16.3	3.2	0.9	49.3	35.4	19.9	0.3	30.4	282
XFeat [30]	85.4	67.4	24.3	5.2	0.9	32.1	2.4	0.1	0.0	34.4	8.3	7.1	0.0	14.2	54
XFeat* [30]	62.4	69.1	27.6	7.6	1.5	32.8	4.5	0.6	0.0	33.8	9.4	9.2	0.0	15.1	82
XFeat+LighterGlue [30]	64.6	91.7	59.1	26.2	8.1	56.6	20.9	4.6	0.2	48.0	33.4	21.4	1.2	30.1	43
<i>Detector-free methods</i>															
LoFTR [35]	87.2	88.4	47.2	17.5	5.0	51.6	10.1	2.3	0.6	43.2	27.9	15.1	0.0	24.9	185
ELoFTR [44]	56.4	90.3	50.8	22.1	6.3	51.2	15.6	4.4	0.7	42.2	30.8	18.2	0.1	26.6	124
ASpanFormer [4]	72.2	72.3	44.5	21.9	7.4	46.0	14.9	6.9	1.6	42.5	27.2	16.0	0.1	24.8	108
RoMa [11]	67.0	98.3	84.5	52.7	20.2	71.2	43.2	26.6	8.3	57.5	56.2	44.1	3.0	47.3	614
DUST3R [43]	81.8	97.4	90.8	58.4	<u>30.4</u>	<u>73.3</u>	<u>57.9</u>	40.1	9.9	<u>67.4</u>	55.3	50.0	<u>35.2</u>	<u>54.8</u>	257
MAS3R [24]	52.0	<u>97.5</u>	<u>89.6</u>	<u>61.0</u>	28.4	71.2	52.3	<u>42.5</u>	<u>13.8</u>	53.5	65.6	54.5	14.1	53.6	173
<i>Relative pose regression</i>															
AlligatOR (Ours)	100.0	89.7	80.2	61.5	44.3	78.4	61.3	43.9	23.2	77.5	<u>62.7</u>	<u>51.3</u>	37.3	60.3	57

across varying degrees of overlap and viewpoint changes. These visualizations provide insights into the geometric understanding acquired by our model. Conversely, the best CroCo model succeeds in reconstructing masked regions for pairs with high overlaps, but completely fails on more difficult pairs.

5.4. Comparison with state-of-the-art on RUBIK

In Tab. 2, we evaluate the performance of AlligatOR fine-tuned for metric relative pose estimation against state-of-the-art methods on RUBIK [26]. Let us highlight that:

- AlligatOR was trained on nuScenes (on scenes that are not part of RUBIK),
- whereas none of the state-of-the-art methods used nuScenes as training set.

This gives an advantage to AlligatOR over the other methods. However, RUBIK allows the evaluation over large ranges of three geometric criteria—overlap, scale ratio and viewpoint angle—which we found interesting. Despite this advantage, we argue that AlligatOR’s performance remains remarkable, as pretraining with CroCo, in contrast, leads to a significant performance drop (see Tab. 1).

With an overall success rate of 60.3%, AlligatOR ranks first. Notably, it significantly outperforms all other methods on the hardest bin across the three geometric criteria, which confirms the advantage of its pretraining on difficult image pairs. While AlligatOR’s training set was highly skewed toward challenging pairs (see Fig. 4), one might expect a performance drop on easier bins. However, this does not happen: for instance, AlligatOR still ranks first for small scale ratios and small viewpoint angles. Finally, AlligatOR is among the fastest methods, as it directly regresses the relative pose rather than producing intermediate correspondences.

5.5. Future Directions

Our results demonstrate the effectiveness of co-visibility segmentation for pre-training. From this idea, we believe that several promising directions can be explored:

1. **Segmentation Formulations:** Investigating different ways to formulate the segmentation task, including binary vs. three-class approaches.
2. **Curriculum Learning:** Experimenting with curriculums that gradually increase the difficulty of training examples to see if this could further improve performance.
3. **Multi-task Learning:** Studying whether jointly training on multiple downstream tasks can leverage the geometric understanding provided by our co-visibility segmentation approach.
4. **Diverse Environments:** Extending AlligatOR to more diverse indoor and outdoor environments beyond autonomous driving scenarios.

6. Conclusion and Future Work

In this paper, we introduced AlligatOR, a novel pre-training approach for binocular vision that reformulates cross-view completion as a co-visibility segmentation task. Unlike CroCo that relies on masked reconstruction, our approach explicitly models co-visibility relationships between image pairs, enabling more effective learning from challenging examples with limited overlap.

We demonstrated the effectiveness of our approach on the relative pose regression task in the autonomous driving scenario, where AlligatOR significantly outperforms CroCo, particularly on challenging scenes with limited overlap between views. This improvement is especially notable using a diverse training set that include pairs with varying degrees of overlap, highlighting the ability of our approach to learn



Figure 6. **Qualitative comparison between CroCo trained on Cub3-50 and Alligat0R.** For each row from left to right: reference image, target image, masked target image, CroCo reconstruction, and Alligat0R segmentations (co-visible, occluded, outside FOV). CroCo struggles with reconstructing regions with limited overlap, while Alligat0R often correctly identifies co-visible, occluded, and outside FOV regions across varying degrees of overlap and viewpoint changes.

and benefit from geometrically challenging examples.

To enable our approach, we created Cub3, a large-scale dataset of 2.5 million image pairs with dense co-visibility annotations derived from the nuScenes dataset. This dataset provides a valuable resource for future research in binocular vision tasks and will be made publicly available.

Our work demonstrates that explicitly modeling co-visibility through segmentation provides a more effective and interpretable approach to binocular vision tasks compared to reconstruction-based methods, paving the way for more robust visual perception systems.

References

- [1] Hangbo Bao, Li Dong, Songhao Piao, and Furu Wei. Beit: Bert pre-training of image transformers. In *International Conference on Learning Representations*. 1
- [2] Holger Caesar, Varun Bankiti, Alex H Lang, Sourabh Vora, Venice Erin Liong, Qiang Xu, Anush Krishnan, Yu Pan, Giancarlo Baldan, and Oscar Beijbom. nuscenes: A multi-modal dataset for autonomous driving. In *Proceedings of the IEEE/CVF conference on computer vision and pattern recognition*, pages 11621–11631, 2020. 4
- [3] Mathilde Caron, Hugo Touvron, Ishan Misra, Hervé Jégou, Julien Mairal, Piotr Bojanowski, and Armand Joulin. Emerging properties in self-supervised vision transformers. In *Proceedings of the IEEE/CVF international conference on com-*

- puter vision, pages 9650–9660, 2021. 1
- [4] Hongkai Chen, Zixin Luo, Lei Zhou, Yurun Tian, Mingmin Zhen, Tian Fang, David Mckinnon, Yanghai Tsin, and Long Quan. Aspanformer: Detector-free image matching with adaptive span transformer. In *European Conference on Computer Vision*, pages 20–36. Springer, 2022. 2, 7
- [5] Ting Chen, Simon Kornblith, Mohammad Norouzi, and Geoffrey Hinton. A simple framework for contrastive learning of visual representations. In *International conference on machine learning*, pages 1597–1607. PmLR, 2020. 1
- [6] Daniel DeTone, Tomasz Malisiewicz, and Andrew Rabinovich. Superpoint: Self-supervised interest point detection and description. In *Proceedings of the IEEE conference on computer vision and pattern recognition workshops*, pages 224–236, 2018. 7
- [7] Siyan Dong, Shuzhe Wang, Shaohui Liu, Lulu Cai, Qingnan Fan, Juho Kannala, and Yanchao Yang. Reloc3r: Large-scale training of relative camera pose regression for generalizable, fast, and accurate visual localization. *arXiv preprint arXiv:2412.08376*, 2024. 1, 2
- [8] Alexey Dosovitskiy, Lucas Beyer, Alexander Kolesnikov, Dirk Weissenborn, Xiaohua Zhai, Thomas Unterthiner, Mostafa Dehghani, Matthias Minderer, Georg Heigold, Sylvain Gelly, et al. An image is worth 16x16 words: Transformers for image recognition at scale. *arXiv preprint arXiv:2010.11929*, 2020. 2
- [9] Johan Edstedt, Ioannis Athanasiadis, Mårten Wadenbäck, and Michael Felsberg. Dkm: Dense kernelized feature matching for geometry estimation. In *Proceedings of the IEEE/CVF Conference on Computer Vision and Pattern Recognition*, pages 17765–17775, 2023. 2
- [10] Johan Edstedt, Georg Bökman, and Zhenjun Zhao. Dedode v2: Analyzing and improving the dedode keypoint detector. In *Proceedings of the IEEE/CVF Conference on Computer Vision and Pattern Recognition*, pages 4245–4253, 2024. 7
- [11] Johan Edstedt, Qiyu Sun, Georg Bökman, Mårten Wadenbäck, and Michael Felsberg. Roma: Robust dense feature matching. In *Proceedings of the IEEE/CVF Conference on Computer Vision and Pattern Recognition*, pages 19790–19800, 2024. 2, 7
- [12] Sven Elflein, Qunjie Zhou, Sérgio Agostinho, and Laura Leal-Taixé. Light3r-sfm: Towards feed-forward structure-from-motion. *arXiv preprint arXiv:2501.14914*, 2025. 1
- [13] Miao Fan, Mingrui Chen, Chen Hu, and Shuchang Zhou. Occ² net: Robust image matching based on 3d occupancy estimation for occluded regions. In *Proceedings of the IEEE/CVF International Conference on Computer Vision*, pages 9652–9662, 2023. 2
- [14] Hugo Germain, Vincent Lepetit, and Guillaume Bourmaud. Visual correspondence hallucination. In *International Conference on Learning Representations*, 2022. 2
- [15] Pierre Gleize, Weiyao Wang, and Matt Feiszli. Silk: Simple learned keypoints. In *Proceedings of the IEEE/CVF international conference on computer vision*, pages 22499–22508, 2023. 2
- [16] Jean-Bastien Grill, Florian Strub, Florent Altché, Corentin Tallec, Pierre Richemond, Elena Buchatskaya, Carl Doersch, Bernardo Avila Pires, Zhaohan Guo, Mohammad Gheshlaghi Azar, et al. Bootstrap your own latent—a new approach to self-supervised learning. *Advances in neural information processing systems*, 33:21271–21284, 2020. 1
- [17] Kaiming He, Xinlei Chen, Saining Xie, Yanghao Li, Piotr Dollár, and Ross Girshick. Masked autoencoders are scalable vision learners. In *Proceedings of the IEEE/CVF conference on computer vision and pattern recognition*, pages 16000–16009, 2022. 1
- [18] Vlad Hondru, Florinel Alin Croitoru, Shervin Minaee, Radu Tudor Ionescu, and Nicu Sebe. Masked image modeling: A survey. *arXiv preprint arXiv:2408.06687*, 2024. 2
- [19] Will Hutchcroft, Yuguang Li, Ivaylo Boyadzhiev, Zhiqiang Wan, Haiyan Wang, and Sing Bing Kang. Covispose: Co-visibility pose transformer for wide-baseline relative pose estimation in 360° indoor panoramas. In *European Conference on Computer Vision*, pages 615–633. Springer, 2022. 2
- [20] Wei Jiang, Eduard Trulls, Jan Hosang, Andrea Tagliasacchi, and Kwang Moo Yi. Cotr: Correspondence transformer for matching across images. In *Proceedings of the IEEE/CVF International Conference on Computer Vision*, pages 6207–6217, 2021. 2
- [21] Linyi Jin, Richard Tucker, Zhengqi Li, David Fouhey, Noah Snavely, and Aleksander Holynski. Stereo4d: Learning how things move in 3d from internet stereo videos. *arXiv preprint arXiv:2412.09621*, 2024. 1
- [22] Alex Kendall, Yarin Gal, and Roberto Cipolla. Multi-task learning using uncertainty to weigh losses for scene geometry and semantics. In *Proceedings of the IEEE conference on computer vision and pattern recognition*, pages 7482–7491, 2018. 4
- [23] Shinjeong Kim, Marc Pollefeys, and Daniel Barath. Learning to make keypoints sub-pixel accurate. In *European Conference on Computer Vision*, pages 413–431. Springer, 2025. 2
- [24] Vincent Leroy, Yohann Cabon, and Jérôme Revaud. Grounding image matching in 3d with mast3r. *arXiv preprint arXiv:2406.09756*, 2024. 1, 2, 7
- [25] Philipp Lindenberger, Paul-Edouard Sarlin, and Marc Pollefeys. Lightglue: Local feature matching at light speed. In *Proceedings of the IEEE/CVF International Conference on Computer Vision*, pages 17627–17638, 2023. 2
- [26] Thibaut Loiseau and Guillaume Bourmaud. Rubik: A structured benchmark for image matching across geometric challenges. *arXiv preprint arXiv:2502.19955*, 2025. 2, 4, 6, 7
- [27] David G Lowe. Distinctive image features from scale-invariant keypoints. *International journal of computer vision*, 60:91–110, 2004. 7
- [28] Maxime Oquab, Timothée Darcet, Théo Moutakanni, Huy Vo, Marc Szafraniec, Vasil Khalidov, Pierre Fernandez, Daniel Haziza, Francisco Massa, Alaaeldin El-Nouby, et al. Dinov2: Learning robust visual features without supervision. *Transactions on Machine Learning Research Journal*, pages 1–31, 2024. 1
- [29] Luigi Piccinelli, Yung-Hsu Yang, Christos Sakaridis, Mattia Segu, Siyuan Li, Luc Van Gool, and Fisher Yu. Unidepth: Universal monocular metric depth estimation. In *Proceed-*

- ings of the *IEEE/CVF Conference on Computer Vision and Pattern Recognition*, pages 10106–10116, 2024. 4
- [30] Guilherme Potje, Felipe Cadar, André Araujo, Renato Martins, and Erickson R Nascimento. Xfeat: Accelerated features for lightweight image matching. In *Proceedings of the IEEE/CVF Conference on Computer Vision and Pattern Recognition*, pages 2682–2691, 2024. 2, 7
- [31] Paul-Edouard Sarlin, Daniel DeTone, Tomasz Malisiewicz, and Andrew Rabinovich. Superglue: Learning feature matching with graph neural networks. In *Proceedings of the IEEE/CVF conference on computer vision and pattern recognition*, pages 4938–4947, 2020. 2
- [32] Johannes L Schonberger and Jan-Michael Frahm. Structure-from-motion revisited. In *Proceedings of the IEEE conference on computer vision and pattern recognition*, pages 4104–4113, 2016. 4
- [33] Brandon Smart, Chuanxia Zheng, Iro Laina, and Victor Adrian Prisacariu. Splatt3r: Zero-shot gaussian splatting from uncalibrated image pairs. *arXiv preprint arXiv:2408.13912*, 2024. 1
- [34] Zikai Song, Run Luo, Junqing Yu, Yi-Ping Phoebe Chen, and Wei Yang. Compact transformer tracker with correlative masked modeling. In *Proceedings of the AAAI conference on artificial intelligence*, pages 2321–2329, 2023. 2
- [35] Jiaming Sun, Zehong Shen, Yuang Wang, Hujun Bao, and Xiaowei Zhou. Loftr: Detector-free local feature matching with transformers. In *Proceedings of the IEEE/CVF conference on computer vision and pattern recognition*, pages 8922–8931, 2021. 2, 7
- [36] Dongli Tan, Jiang-Jiang Liu, Xingyu Chen, Chao Chen, Ruixin Zhang, Yunhang Shen, Shouhong Ding, and Rongrong Ji. Eco-tr: Efficient correspondences finding via coarse-to-fine refinement. In *European Conference on Computer Vision*, pages 317–334. Springer, 2022.
- [37] Shitao Tang, Jiahui Zhang, Siyu Zhu, and Ping Tan. Quadtree attention for vision transformers. In *International Conference on Learning Representations*, 2022. 2
- [38] Prune Truong, Martin Danelljan, Radu Timofte, and Luc Van Gool. Pdc-net+: Enhanced probabilistic dense correspondence network. *IEEE Transactions on Pattern Analysis and Machine Intelligence*, 45(8):10247–10266, 2023. 2
- [39] Michał Tyszkiewicz, Pascal Fua, and Eduard Trulls. Disk: Learning local features with policy gradient. *Advances in Neural Information Processing Systems*, 33:14254–14265, 2020. 7
- [40] Hengyi Wang and Lourdes Agapito. 3d reconstruction with spatial memory. *arXiv preprint arXiv:2408.16061*, 2024. 1
- [41] Qing Wang, Jiaming Zhang, Kailun Yang, Kunyu Peng, and Rainer Stiefelwagen. Matchformer: Interleaving attention in transformers for feature matching. In *Proceedings of the Asian Conference on Computer Vision*, pages 2746–2762, 2022. 2
- [42] Qianqian Wang, Yifei Zhang, Aleksander Holynski, Alexei A Efros, and Angjoo Kanazawa. Continuous 3d perception model with persistent state. *arXiv preprint arXiv:2501.12387*, 2025. 1
- [43] Shuzhe Wang, Vincent Leroy, Yohann Cabon, Boris Chidlovskii, and Jerome Revaud. Dust3r: Geometric 3d vision made easy. In *Proceedings of the IEEE/CVF Conference on Computer Vision and Pattern Recognition*, pages 20697–20709, 2024. 1, 2, 7
- [44] Yifan Wang, Xingyi He, Sida Peng, Dongli Tan, and Xiaowei Zhou. Efficient loftr: Semi-dense local feature matching with sparse-like speed. In *Proceedings of the IEEE/CVF Conference on Computer Vision and Pattern Recognition*, pages 21666–21675, 2024. 2, 7
- [45] Philippe Weinzaepfel, Vincent Leroy, Thomas Lucas, Romain Brégier, Yohann Cabon, Vaibhav Arora, Leonid Antsfeld, Boris Chidlovskii, Gabriela Csurka, and Jérôme Revaud. Croco: Self-supervised pre-training for 3d vision tasks by cross-view completion. *Advances in Neural Information Processing Systems*, 35:3502–3516, 2022. 1, 2, 5
- [46] Philippe Weinzaepfel, Thomas Lucas, Vincent Leroy, Yohann Cabon, Vaibhav Arora, Romain Brégier, Gabriela Csurka, Leonid Antsfeld, Boris Chidlovskii, and Jérôme Revaud. Croco v2: Improved cross-view completion pre-training for stereo matching and optical flow. In *Proceedings of the IEEE/CVF International Conference on Computer Vision*, pages 17969–17980, 2023. 1, 2, 4
- [47] Jianing Yang, Alexander Sax, Kevin J Liang, Mikael Henaff, Hao Tang, Ang Cao, Joyce Chai, Franziska Meier, and Matt Feiszli. Fast3r: Towards 3d reconstruction of 1000+ images in one forward pass. *arXiv preprint arXiv:2501.13928*, 2025. 1
- [48] Lihe Yang, Bingyi Kang, Zilong Huang, Zhen Zhao, Xiaogang Xu, Jiashi Feng, and Hengshuang Zhao. Depth anything v2. *arXiv preprint arXiv:2406.09414*, 2024. 4
- [49] Botao Ye, Sifei Liu, Haoifei Xu, Xueting Li, Marc Pollefeys, Ming-Hsuan Yang, and Songyou Peng. No pose, no problem: Surprisingly simple 3d gaussian splats from sparse unposed images. *arXiv preprint arXiv:2410.24207*, 2024. 1
- [50] Junyi Zhang, Charles Herrmann, Junhwa Hur, Varun Jampani, Trevor Darrell, Forrester Cole, Deqing Sun, and Ming-Hsuan Yang. Monst3r: A simple approach for estimating geometry in the presence of motion. *arXiv preprint arXiv:2410.03825*, 2024. 1
- [51] Haojie Zhao, Dong Wang, and Huchuan Lu. Representation learning for visual object tracking by masked appearance transfer. In *Proceedings of the IEEE/CVF conference on computer vision and pattern recognition*, pages 18696–18705, 2023. 2
- [52] Xiaoming Zhao, Xingming Wu, Weihai Chen, Peter CY Chen, Qingsong Xu, and Zhengguo Li. Aliked: A lighter keypoint and descriptor extraction network via deformable transformation. *IEEE Transactions on Instrumentation and Measurement*, 72:1–16, 2023. 2, 7
- [53] Jinghao Zhou, Chen Wei, Huiyu Wang, Wei Shen, Cihang Xie, Alan Yuille, and Tao Kong. Image bert pre-training with online tokenizer. In *International Conference on Learning Representations*. 1
- [54] Shengjie Zhu and Xiaoming Liu. Pmatch: Paired masked image modeling for dense geometric matching. In *Proceedings of the IEEE/CVF Conference on Computer Vision and Pattern Recognition*, pages 21909–21918, 2023. 2



Alligat0R: Pre-Training through Co-Visibility Segmentation for Relative Camera Pose Regression

Supplementary Material

7. Supplementary Material

In this supplementary material, we provide additional details about our Alligat0R model, including training curves and visualizations that didn't fit in the main paper but may be of interest to readers.

7.1. Pre-training Learning Curves

Figure 7 shows the learning curves for the pre-training phase of both CroCo and Alligat0R on the Cub3-50 and Cub3-all datasets. As can be observed, Alligat0R's loss converges smoothly on both datasets, indicating stable training. There are fewer number of steps for CroCo as we have a batch size of 64 per GPU, compared to Alligat0R where we have a batch size of 32.

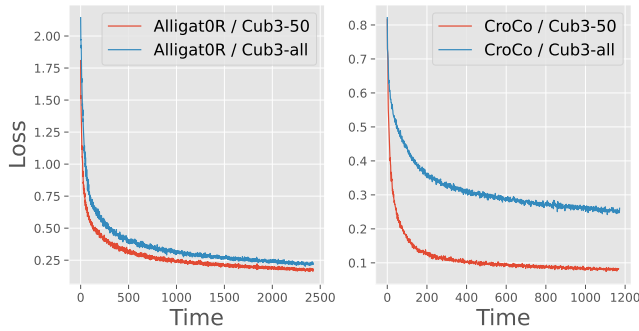


Figure 7. Learning curves during pre-training for CroCo (reconstruction loss) and Alligat0R (segmentation loss) on Cub3-50 and Cub3-all datasets. Alligat0R shows stable convergence on both datasets, while CroCo exhibits instability on the more challenging Cub3-all dataset which contains image pairs with lower overlap.

7.2. Fine-tuning Learning Curves

Figure 8 presents the fine-tuning curves for the pose regression task. The plots show the pose loss during training. Alligat0R fine-tuned on Cub3-all shows faster convergence and reaches higher accuracy than the same configuration for CroCo, highlighting the transferability of features learned through co-visibility segmentation on difficult pairs.

7.3. Detailed Performance

Figure 9 provides a more detailed breakdown of performance across different geometric criteria than what was presented in the main paper. This visualization further emphasizes Alligat0R's strong performance across all difficulty

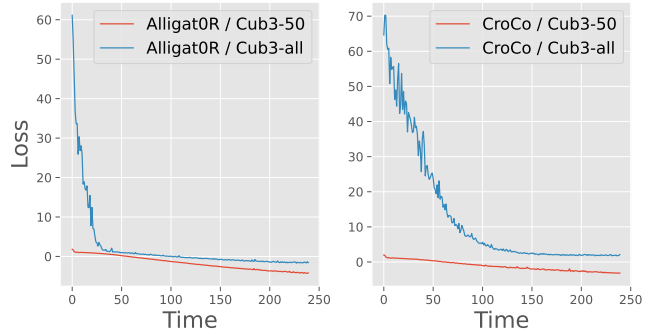


Figure 8. Learning curves during fine-tuning for pose regression. Alligat0R pre-trained on Cub3-all converges faster and achieves higher success rates than other methods, demonstrating the effectiveness of our co-visibility segmentation pre-training approach.

ranges, especially on very difficult scenarios where traditional methods struggle.

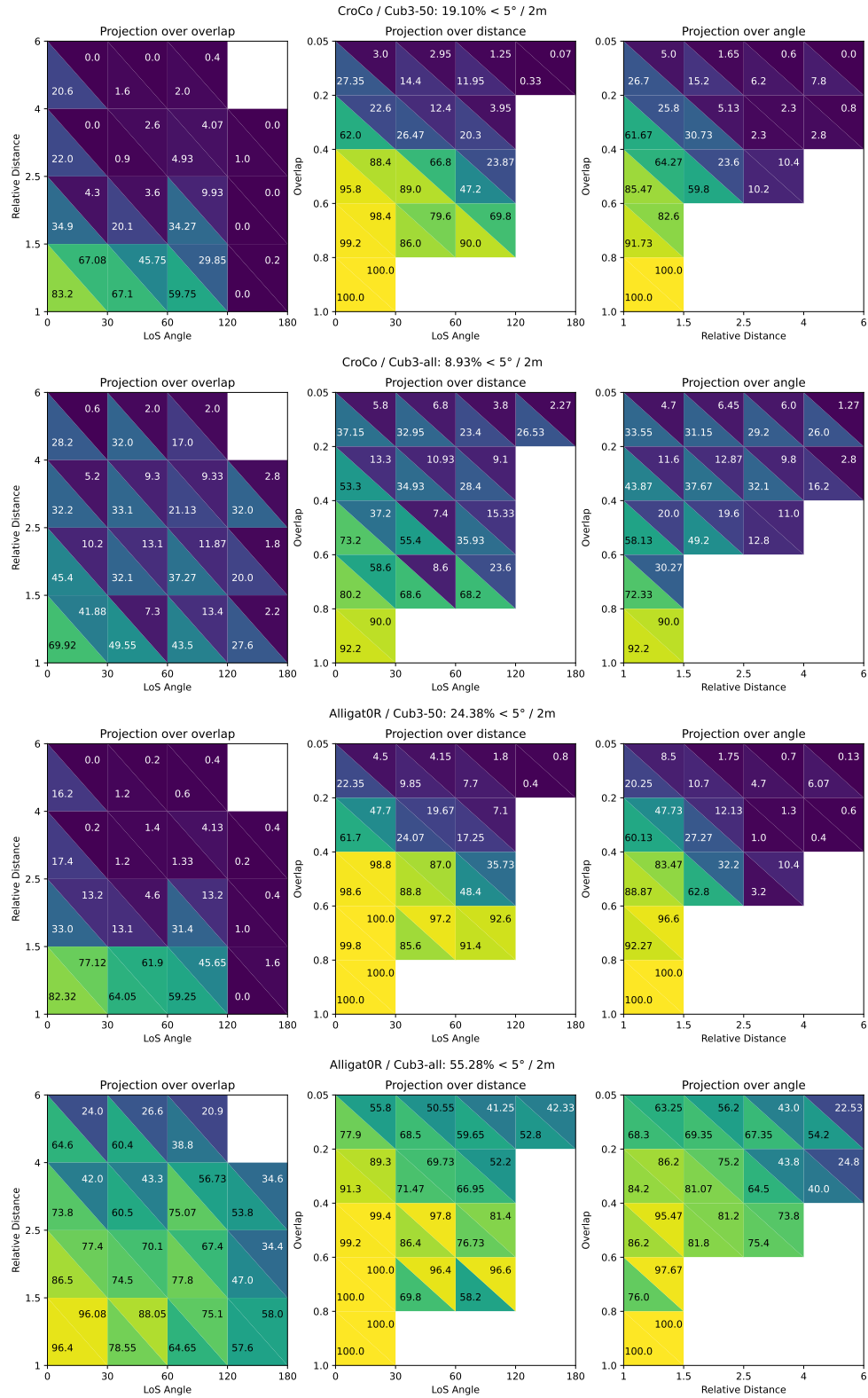


Figure 9. **Detailed breakdown of performance across different geometric criteria.** Success rate either for $R@5^\circ$ or $t@2m$ (bottom-left and top-right of each triangle, respectively), when projecting results onto individual geometric criteria of RUBIK. For each method, we show three plots corresponding to the projection over overlap (left), scale ratio (middle), and viewpoint angle (right)